Available online at www.sciencedirect.com
SCIENCE DIRECT®
Microporous and Mesoporous Materials 77 (2005) 215–221
MICROPOROUS AND MESOPOROUS MATERIALS
www.elsevier.com/locate/micromeso

Study of cancrinite-type zeolites as possible antacid agents

Carlos F. Linares [a,*], Selene Sánchez [a], Caribay Urbina de Navarro [b], Karina Rodríguez [c], Mireya R. Goldwasser [c]

[a] *Laboratorio de Catálisis y Metales de Transición, Facultad de Ciencias y Tecnología, Departamento de Química, Universidad de Carabobo, Valencia, Edo, Carabobo, Apartado Postal 3336, Venezuela*
[b] *Centro de Microscopía Electrónica, Escuela de Biología, Av. Los Ilustres, Los Chaguaramos, UCV, Caracas, Venezuela*
[c] *Centro de Catálisis, Petróleo y Petroquímica, Facultad de Ciencia, Escuela de Química, Av. Los Ilustres, Los Chaguaramos, UCV, Caracas 1020A, Venezuela*

Received 23 February 2003; received in revised form 23 August 2004; accepted 23 August 2004

Abstract

A series of carbonated–nitrated cancrinite-type zeolites were synthesized using X zeolite as silicon and aluminum source and metallic cations such as magnesium, aluminum and their mixture as templates. The synthesized solids were characterized by means of techniques such as XRD, FT-IR, UV–visible, DTGA, BET surface area and chemical analysis. The XRD analysis confirmed the presence of cancrinite-type zeolite without the presence of other phases. The solids were tested in a synthetic gastric juice simulating condition of hyperacidity. Small doses of solids were enough to adjust the pH of the system. These results were compared to those obtained with a commercial hydrotalcite based drug. Both solids showed comparable results. Additionally, the solid–pepsin interaction was also evaluated among the synthesized cancrinite-type zeolites.

Keywords: Cancrinite; Antacid; Carbonated zeolites; Nitrated zeolites; Al; Mg

1. Introduction

Cancrinite are one of most rare members of the feldspathoid group, classified as such due to its low silicon content. However, cancrinite is classified also as a zeolite, due to its open pore structure, which confers molecular sieve properties [1]. There are few regions where cancrinite zeolite can be found as natural ores such as in Kola peninsula, Russia; Iron Hill, Colorado, USA; India; Finland and the Fen region in Norway.

The structure of cancrinite-type zeolites is based on periodical array of small cages (ε cages) distributed in the hexagonal structure and a big channel of 12 rings along the direction of the hexagonal *c*-axis of the structure forming one-dimensional rectilineous channels along the *c*-axis. Access to these channels occurs through windows formed by 12 member rings. Clusters of $Na–H_2O^+$ are found inside the ε cages, which generate extra structural excess of positive charge. This positive charge must be compensated by extra framework anions placed in the interior of the main channels along the *c*-axis [1]. Carbonates, nitrates, chlorides, sulfates and hydroxides are among the anions present [2,3]. However, the synthesis of cancrinite-type zeolites with anions such as sulfurs, thiosulfates, sulfites and selenates have also been reported [4].

Generally, complex procedures of temperature, pressure and crystallization are used to synthesize cancrinite-type zeolites [5,6]. However, using X zeolite as

* Corresponding author. Fax: +58 241 8678805.
E-mail address: clinares@thor.uc.edu.ve (C.F. Linares).

1387-1811/$ - see front matter © 2004 Elsevier Inc. All rights reserved.
doi:10.1016/j.micromeso.2004.08.030

aluminum and silicon source, we achieved the synthesis of carbonated–nitrated cancrinite-type zeolites under highly improved experimental parameters [7].

Due to blockage of the main zeolite channels by anions present in the structure, no many applications are reported concerning cancrinite zeolites. However, the presence of carbonate could make them suitable as antacid. Rivera et al. [8], in an interesting work, modified purified natural clinoptilolite zeolites with sodium carbonate obtaining an effective antacid against stomach hyperacidity. The drawback of these natural types of zeolites is its purification and homogenization.

It is expected that cancrinite-type zeolites act as an effective antacid due to its low silicon–aluminum ratio (Si/Al = 1) and to the presence of carbonate anions. Its major advantage is the fact that carbonate anions are trapped inside the zeolite channels allowing the release of carbonate as the neutralization reaction proceeds without a "rebound effect" usually produced by sodium carbonate based antacid.

In this work, carbonated–nitrated cancrinite-type zeolites were synthesized. These solids were tested as antacid in synthetic gastric juice simulating hyperacidity conditions. Results are compared to those obtained with a commercial hydrotalcite based drug. Additionally, the solid–pepsin interaction was also evaluated since this enzyme plays an important role in the digestive properties of the stomach.

2. Experimental

2.1. Synthesis of cancrinite-type zeolites

The carbonated–nitrated cancrinite-type zeolites were synthesized according to the previously reported procedure [7] using a previously characterized X zeolite (ZX, Strem Chemicals, Si/Al = 1.3). 0.5 grams of the faujasite-type zeolite were impregnated with three times the volume needed for incipient impregnation (4 ml/g) using some of the gels described in Table 1. Those gels were prepared by mixing up two solutions: solution A, consisting of a mixture of Na_2CO_3 and NaOH in concentrations of 1.33 M and 4.63 M respectively, and solution B containing $Mg(NO_3)_2 \cdot 6H_2O$ and/or $Al(NO_3)_3 \cdot 9H_2O$ in concentrations of 1.10 M and 0.376 M respectively. The gel was prepared by adding very slowly from solution B to solution A under constant stirring as specified on Table 1.

Table 1
Impregnation of X zeolites with gels prepared as specified

Zeolite	NaOH and Na_2CO_3	$Mg(NO_3)_2 \cdot 6H_2O$	$Al(NO_3)_3 \cdot 9H_2O$
Can(AlMg)	+	+	+
Can(Mg)	+	+	–
Can(Al)	+	–	+

(+) The reactant is found in the reaction gel; (–) the reactant is not found in the reaction gel.

The impregnated zeolites were placed in a Teflon container without agitation at autogenous pressure and in a convection oven at 80 °C and 27 h. After that time the solids were washed with abundant water until a pH ≅ 7.

To ascertain the effectiveness of the synthesized carbonated–nitrated cancrinite zeolite as antacid, their behavior was compared to that of a Bayer commercial antacid (Baytalcid®) based on hydrotalcites as active agent.

2.2. Characterization

Solids were characterized by chemical analysis, XRD, BET surface area, FT-IR and DTGA. XRD studies were conducted using a Phillips PW 3442 diffractometer with a CoKα radiation (1.54060 Å) for crystalline phase detection between 4° and 80° (2θ), and the patterns obtained were compared with JCPDS data files. Physisorption measurements were performed with a Beckman Coulter SA 3100 instrument; BET surface areas were determined by nitrogen adsorption at −196 °C with an Ar/N_2 ratio of 70/30. The presence of functional groups and evaluation of purity of solids were achieved by FT-IR; spectra were recorded in a Perkin-Elmer 283 spectrometer in the 2000–200 cm^{-1} range. Samples were prepared dissolving the solids in KBr to form a thin pastille. Differential thermogravimetric analysis (TGA) was performed to evaluate the nitrate and carbonate content. Samples were placed in Pt sample holders and heated from 25 to 1000 °C at 10 °C/min in a nitrogen flow. Metal concentration on the synthesized cancrinite zeolites was determined by plasma atomic emission using a Varian Techtron A.A.6. Previous to the analysis, the solids were fused with lithium metaborate and dissolved in HNO_3 (10% v/v).

2.3. Antacid capacity

The antacid capacity of the synthesized zeolites was evaluated using the methodology previously reported by Rivera et al. [9]. Solids were tested in a synthetic gastric juice (HCl + pepsin, pH ≈ 1.5), contacting 50–500 mg of the solids with an aliquot of 20 ml of the synthetic gastric juice. This dispersed solution was shaken during 1 h at 37 °C to simulate the rhythmical movements of the stomach. The solution was then filtered and an aliquot of 10 ml was potentiometrically titrated with previously standardized NaOH; using an Acumment AB15 pH meter with glass electrode and a sensitivity of ±0.05 pH units. The pH of the solutions was evaluated in two ways: (a) directly, using the previously calibrated pH meter, named "experimental pH", (b) the pH

determined by the potentiometer titration (theoretical pH = $-\log[H^+]$), where $[H^+]$ corresponds to the free protons concentration determined in the acid–base titration.

The interaction solid–pepsin was measure by UV–visible spectroscopy by means of a HP 8452A with diode arrangement, using 400 mg of the zeolite mixed with the synthetic gastric juice. After separation by filtration, an aliquot was analyzed and the spectrum was recorded between 200 and 400 nm. Spectra were taken before and after contacting the solids with the synthetic gastric juice.

3. Results and discussion

The XRD analysis (Figs. 1 and 2) showed reflections attributed to the cancrinite zeolite, consistent with P_{63} spatial group [10]. No other phases such as sodalite were present in the synthesized samples. However, the presence of a small peak, signaled with an asterisk, in the Can(Mg) and Can(AlMg) zeolites could be attributed to the (1 1 1) reflection of the unconverted precursor material (X zeolite). The absence of this peak on the Can(Al) zeolite pattern indicates the complete conversion of the precursor zeolite.

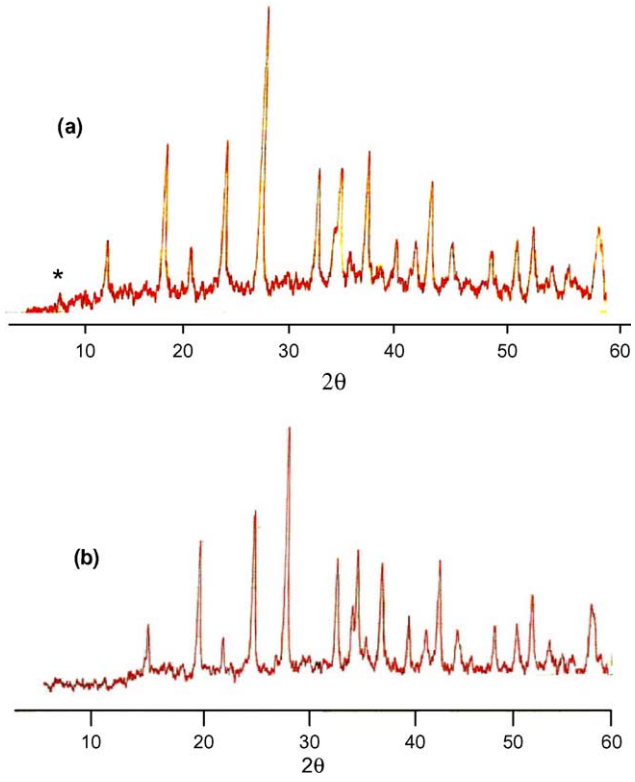

Fig. 1. XRD analysis of (a) Can(AlMg) and (b) Can(Al) cancrinite-type zeolites. Asterisk represents a possible phase from X zeolite.

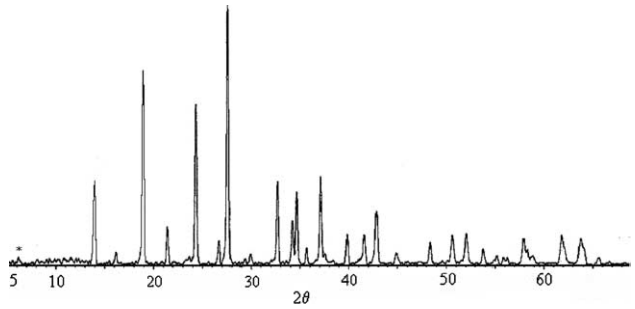

Fig. 2. XRD analysis of Can(Mg) cancrinite-type zeolite. Asterisk represents a possible phase from X zeolite.

FT-IR spectra of the synthesized zeolites using different reaction gels are shown in Fig. 3(a)–(c). Bands placed at 1446 cm^{-1} and 1424 cm^{-1} could be assigned to the presence of nitrates and carbonates anions occluded in the internal cavities of the cancrinite zeolite. Because both anions show bands in the same region of the spectra, their identification based only in their IR spectra, is difficult. Carbonates bands appear in the 1410–1455 cm^{-1} region [11] while nitrate has been identified between 1380 and 1440 cm^{-1} [12]. The band observed at 1630 cm^{-1}, present in all spectra, corresponds to water molecules occluded inside the cancrinite structure [13]. Bands in the 1100–600 cm^{-1} region correspond to symmetric and asymmetric vibrations of the atoms that form the structural units of the zeolite. Those bands are considered as the fingerprint of the zeolite, specially the asymmetric vibrations between 685 cm^{-1} and 344 cm^{-1} [14]. All synthesized zeolites, show bands in the previously describe regions corresponding to those

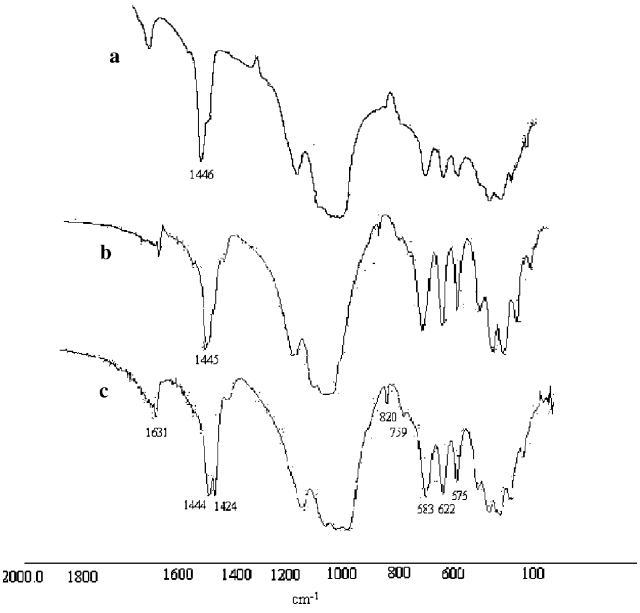

Fig. 3. FT-IR spectra of synthesized cancrinite-type zeolites: (a) Can(Mg), (b) Can(Al) and (c) Can(AlMg).

attributed to the cancrinite structure; especially Can(Al) zeolite, which shows well-defined bands. For Can(Mg) and Can(AlMg) zeolites, bands are less well-defined probably due to the presence of traces of unconverted X zeolite.

Thermogravimetric analysis of the samples are shown in Figs. 4–6. Two well-defined regions are observed. The first region between 140 °C and 390 °C is associated to water loss from the ε cages of the cancrinite. The second region at temperatures higher than 390 °C associated to loss of superstructure of the material and to the evolution of nitrate and carbonate ions from the cancrinite. According to Barrer et al. [2] nitrate ions are loss as nitrogen oxide and oxygen at 800 °C. Hackbarth et al. [15] reported carbonate ions evolution from sodium carbonate as carbon dioxide and sodium oxide at temperatures higher (~900 °C). Differences are observed in the first region: for Can(AlMg) (Fig. 4) zeolite, two peaks were obtained, named I (185 °C) and II (344 °C). Different coordination form of water molecules inside the ε cages has been claimed [1]. The first peak corresponds to water loss from the cluster $[Na \cdot H_2O]^+$ with longer bond distance between Na^+ and H_2O. The second peak corresponds to loss of water coordinated to Na^+ with shorter bond distance. Those peaks are not well defined for Can(Al) zeolite (Fig. 5), instead a broad band with a maximum at 219 °C was observed, indicating that on this zeolite there is not a clear difference regarding the coordination of water to sodium ions, as previously established. While for Can(Mg) zeolite (Fig. 6), only one peak at 352 °C was shown, indicating that one type only of water molecule is present, attributed to water molecules coordinated to sodium ions by short bonds [1]. However, further microstructure analysis should be carried out to understand the existence of different modes of water coordination Na^+ for similar zeolites.

The DTGA analysis at higher temperature ($T > 390$ °C) also showed differences depending on the zeolite. As can be observed for Can(AlMg) zeolite,

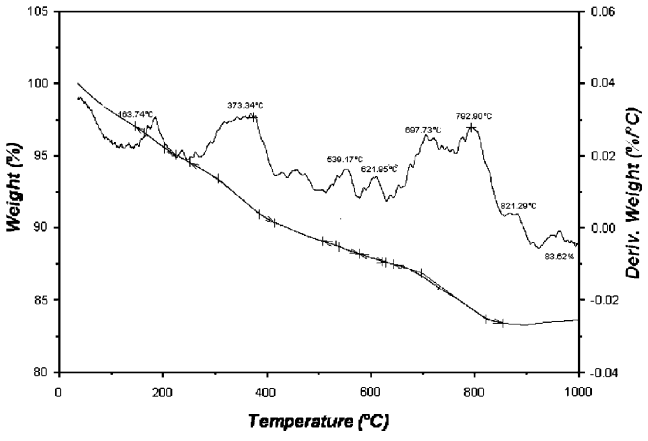

Fig. 4. DTGA of Can(AlMg).

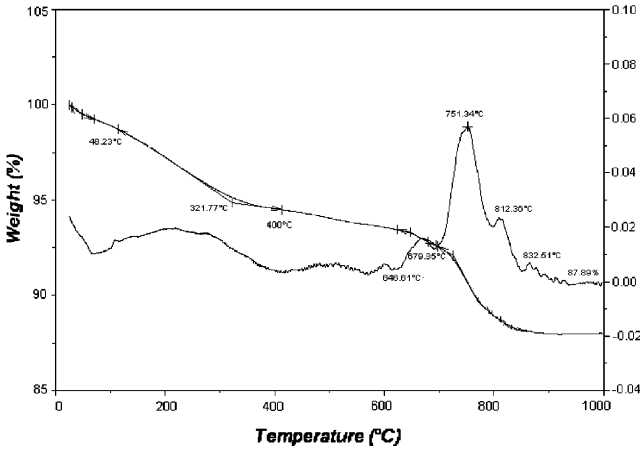

Fig. 5. DTGA of Can(Al).

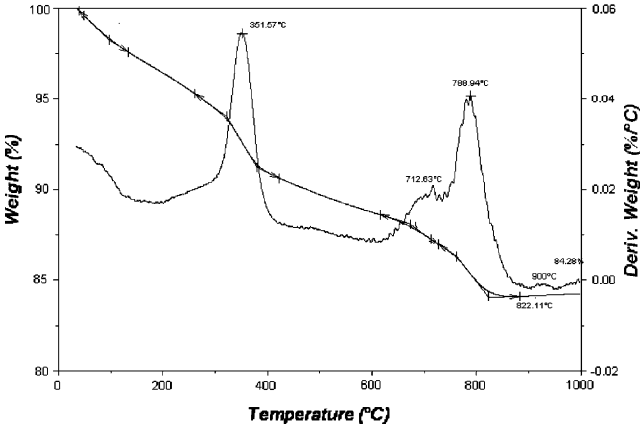

Fig. 6. DTGA of Can(Mg).

two small peaks appear at 537 and 615 °C. These peaks correspond to the collapse of the structure, as previously reported [1]. However, the presence of two peaks is surprising. Even that there is not a clear explanation for this behavior, the presence of two types of cancrinite with different incorporated anions to the structure (carbonate, nitrate or both) is not discarded. However, the detection of the simultaneous existence of more than one type of cancrinite zeolites with similar incorporated anions was not possible by means of IR and XRD analysis. Even that nitrate ions should leave the zeolites at one temperature, two peaks at 706 and 792 °C were observed for the evolution of nitrates. Again the presence of two type of cancrinite zeolite is claimed for this behavior. The peak at 886 °C could be assign to loss of carbonate ions, which decompose at a higher temperature. These carbonate ions could be sharing one of the cancrinite zeolite with the nitrate ions. Even that there is not a clear definition for all peaks, which difficult their quantification, the size of the observed areas in the thermogram indicate that the concentration of nitrates is higher than that of carbonates. For Can(Mg) zeolite

two peaks only are observed: the smaller at 718 °C and the larger at 789 °C. This last peak is wider and extends up to 822 °C. Again, the first peak corresponds to the collapse of the structure and the second one to the evolution of nitrate (788 °C) and carbonate ions (starting at 800 °C). Interpretation of the thermogram of Can(AlMg) and Can(Mg) zeolites is complex due to the presence of unconverted X zeolite, as established by IR and XRD analysis.

Can(Al) zeolite showed three peaks in the high temperature region: the first one due to loss of superstructure of the cancrinite zeolite (672 °C), the second at 753 °C corresponding to the evolution of nitrate ions and a small peak at 810 °C which could be overlapped by the previous one, corresponding to the evolution of carbonate ions. In conclusion, we observed:

(i) Water loss in this zeolite occurred between 140 and 390 °C, probably due to the presence of water with different types of coordination to the structure.
(ii) A peak due to the collapse of the superstructure of the cancrinite zeolite is observed before the evolution of the nitrate and carbonate ions.
(iii) The evolution of nitrate and carbonate ions is overlapped in the thermogram which difficult their quantification.

Table 2 shows the chemical analysis, BET specific surface area and empirical formula for the synthesized cancrinites. Within experimental error, an excellent correlation between the Si/Al ratio of the reported and synthesized cancrinites is observed. These results together with the FT-IR and XRD analysis confirm the synthesis of the cancrinite-type zeolites. The absence of magnesium or of an excess of aluminum in the chemical analysis indicates that these metals act as templates [9].

As can be observed (Table 2), the surface areas of the synthesized cancrinite are smaller than that of X zeolite. This fact corroborates the effective blockage of the pores by the presence of carbonate ions [16]. These anions are difficult to remove from the cancrinite structure and are the base of the acidity study. Can(AlMg) and Can(Mg) zeolites showed higher surface areas than Can(Al) and the reported cancrinite zeolites. These differences are attributed to the presence of unconverted X zeolite, as observed by IR and XRD analysis. TGA was not conclusive with regard to nitrate and carbonate content inside the structure, which make impossible to propose a definitive chemical formula. Fig. 7 shows the neutralization capacity as a function of zeolite mass for Can(Al) cancrinite zeolite. In general, the behavior of all zeolites is similar, inclusive for the Baytalcid® solid used as reference: the pH increases as the weight of the studied solid increases. For all cases, it was observed that the experimental pH value was higher than that of the theoretical one. This could be attributed to the fact that when using the zeolites the glass electrode is only sensitive to the amount of free protons in the synthetic gastric juice. However, during the neutralization with NaOH (theoretical pH), both neutralization and buffer solutions could be formed by interaction with the pepsin dissolved in the reaction media. Rivera et al. reported similar results [8,9]. These authors suggested the use of the experimental pH as the more effective way to determine the neutralization capacity of zeolites.

Fig. 8 shows the results of experimental pH as a function of mass of the synthesized cancrinite zeolite and of commercial Baytalcid® used as reference. It is observed that as the amount of zeolite increases the neutralization capacity also increases, as previously observed in Fig. 7 for Can(Al) zeolite.

Can(AlMg) and Can(Al) cancrinite-type zeolites neutralize a smaller quantity of protons compared to Can(Mg) zeolite and Baytalcid®. The lower neutralization capacity shown by the two first zeolites is attributed to their low carbonate ions occluded in the zeolite cavities which are responsible for the neutralizing capacity. As expected, on Can(AlMg) zeolite, the carbonate

Table 2
Chemical analysis, BET specific surface area and empirical formula of synthesized cancrinites-type zeolites

Zeolites	Si/Al ratio	Empirical formulae	BET surface area (m^2/g)
X zeolite	1.28	$Na_{84.21}(Si_{107.78}Al_{84}O_{384})$	624
Reported cancrinite [8]	1.00	$Na_8(Si_6Al_6O_{24})CO_3$	9.6
Can(Mg)	0.99	$Na_{6.57}(Si_{5.97}Al_{6.03}O_{24})(NO_3)_x(CO_3)_y$[a]	62
Can(Al)	1.04	$Na_{6.41}(Si_{6.11}Al_{5.88}O_{24})(NO_3)_x(CO_3)_y$[b]	12
Can(AlMg)	1.04	$Na_{6.41}(Si_{6.11}Al_{5.88}O_{24})(NO_3)_x(CO_3)_y$[b]	93

[a] $x + y = 0.54$.
[b] $x + y = 0.53$.

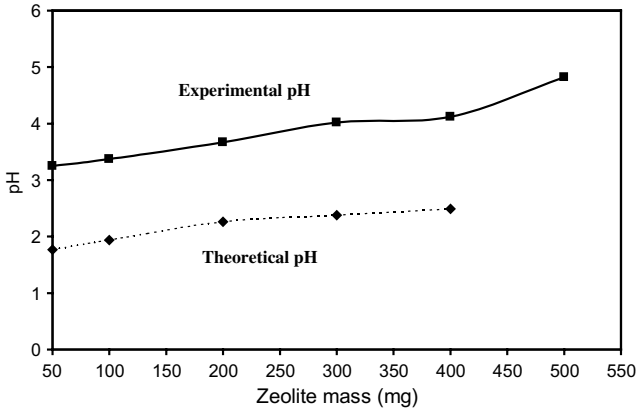

Fig. 7. Theoretical and experimental pH as a function of zeolite mass for Can(Al) cancrinite.

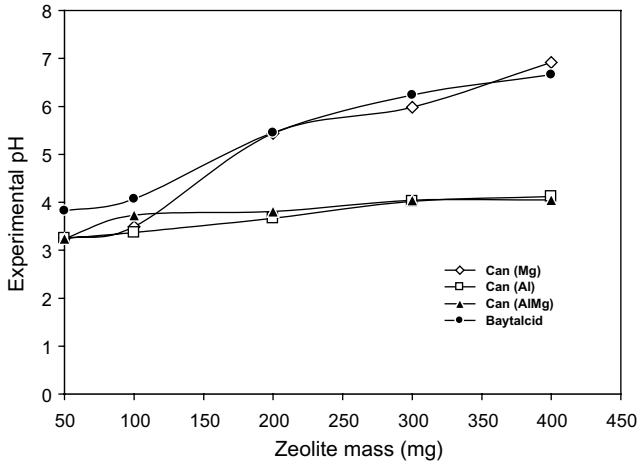

Fig. 8. Experimental pH as a function of cancrinite mass and commercial antacid Baytalcid®.

content is lower than that of the other two zeolites, since nitrate concentration in the starting gel was higher for this zeolite. For Can(Al) zeolite, the lower neutralization capacity could also be related to its lower surface area inhibiting a strong interaction with the protons of the synthetic stomach juice.

Can(Mg) cancrinite zeolite and commercial Baytalcid® solid showed the highest antacid activities, being their behavior similar, especially in the presence of a high mass of both materials. The high antacid capacity of the Can(Mg) zeolite can be attributed to a higher presence of carbonate ions and to its higher surface area compared to other cancrinite zeolite, favoring a stronger interaction with the free protons in the synthetic gastric juice.

The observed similarity between antacid capacity of Can(Mg) zeolite and commercial Baytalcid® looks very promising since it is known that the active component of this solid is hydrotalcite, an anionic clay based on Al, Mg and anions such as carbonates and nitrates which act as counter-ions. This compound is of ample use as antacid due to the ease of Al and Mg to form buffer type equilibrium with protons of the gastric juice, inhibiting sudden increases of the pH of the gastric juice, pH avoiding the so-called ''rebound effect'', usually observed with sodium carbonate based antacids. The fact that Can(Mg) cancrinite zeolite showed a similar effect as Baytalcid® commercial antacid could be pictured as if the cancrinite acts as a carbonate ions reservoir (occluded in the zeolite channels) that are released slowly as the neutralization of the acidity of the gastric juice proceeds.

Similarly, it is well-known that the enzymatic function of the pepsin is highly influenced by the pH of the gastric juice of the stomach. Piper and Fenton [17] indicate that extreme acidity or basicity of the gastric juice denaturalize the enzymatic activity of the pepsin, which shows its higher activity at a pH = 2. At pH = 5 the enzyme starts to deactivate; from a pH = 7, the enzyme irreversibly lesser its activity. However, Fordtran et al. [18] reported that it is possible to obtain therapeutic effects against the acidity if the pH of the stomach juice is not higher than 5 to preserve the activity of the pepsin enzyme. From Fig. 8, it is observed that doses as small as 50 mg of cancrinite zeolite and Baytalcid® are enough to reach the optimum pH necessary to control the hyperacidity of the stomach and to maintain a high enzymatic activity of the pepsin. Quantities higher than 100 mg of Can(Al) cancrinite zeolite and of Baytalcid® are not recommended. Even that they show extraordinary therapeutic properties on the control of the acidity, high doses reduce the enzymatic activity of the pepsin. For Can(Al) and Can(AlMg) cancrinite zeolites, doses as high as 400 mg are possible since the experimental pH was never higher than 4, which is an acceptable acidity for a good enzymatic activity.

The use of low doses of cancrinite-type zeolites to produce effective antacid is an important achievement, since in that way, costs of production will be lower. Contrary to the results observed with the cancrinite zeolite, when antacids are produced from natural zeolites by hydrothermal treatment with Na_2CO_3, as is the case for clinoptilolite zeolite, higher doses (>400 mg) are needed to control hyperacidity [9].

To determine the interaction of the synthesized solids with pepsin, a high quantity of solid (400 mg) was placed in contact with the synthetic gastric juice. Fig. 9 shows the UV–visible spectra of synthesized cancrinite zeolite before and after interaction with synthetic gastric juice. The HCl dissolved pepsin, without interaction with any solid, showed a maximum at 272 nm. After interaction with the cancrinite zeolite, a small decrease in the maximum absorbance of the pepsin was observed, especially for Can(AlMg) cancrinite zeolite. This small decrease is probably due to its higher surface area that favors a stronger interaction with the enzymes. However, no solid showed a different spectrum to that of the original

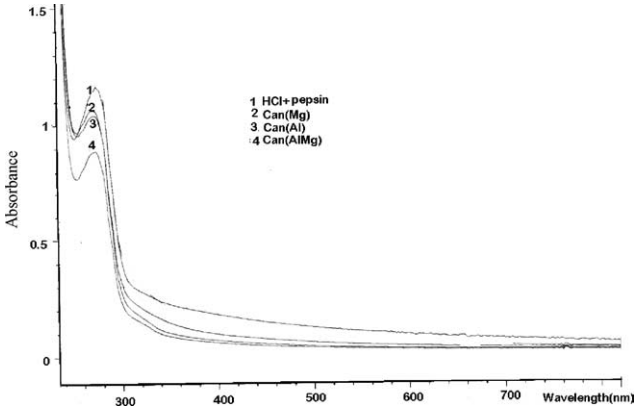

Fig. 9. UV–visible spectra of synthesized cancrinite-type zeolites before and after interaction with synthetic gastric juice.

pepsin. Evidently, there was not a chemical reaction between the enzyme and the solids, but only some adsorption occurs on the surface of the solids. However, this interaction must be very weak to preserve the enzymatic activity. It is important to point out that these tests were performed using high quantities of the solids. When using doses at which our system will work (50 mg); the interactions will be even weaker. These results remark the possibility of using these solids as promising effective antacids.

4. Conclusions

It is possible to use synthesized carbonated–nitrated cancrinite-type zeolites as effective antacid drugs. It was observed that the effectiveness of the cancrinite-type zeolite depends on parameters such as surface area and the amount of carbonate anions present in the solid. Neutralization tests indicate that doses as small as 50 mg of the zeolite increase the pH to normal acidity conditions of the stomach juice, without denaturalization of the pepsin enzymatic protein. The interaction zeolite–enzyme was not significant as established by the low zeolite's mass used. The low doses needed to neutralize hyperacidity make these solids promising as commercial effective antacids.

Acknowledgment

Authors are grateful to FONACIT F-2001000774, CDCH-UC and CDCH-UCV project no. 03-12-4657-2000 for financial support. We also acknowledge the insightful comments of Prof. Gilbert Pinto.

References

[1] I. Hassan, H.D. Grundy, Can. Mineral. 29 (1991) 49.
[2] R.M. Barrer, J.F. Cole, J. Chem. Soc. (A) (1970) 1516.
[3] H.D. Grundy, I. Hassan, Can. Mineral. 20 (1982) 239.
[4] G.-G. Lindner, K. Hoffmann, K. Witke, D. Reiner, Ch. Heinnemann, W. Koch, J. Solid State Chem. 126 (1996) 50.
[5] M. Barnes, J. Addai-Mensah, A. Gerson, Coll. Surf. A: Physicochem.. Eng. Aspects 157 (1999) 101.
[6] C. Liu, S. Li, K. Tu, R. Xu, J. Chem. Soc., Chem. Comm. (1993) 1645.
[7] C.F. Linares, S. Madriz, M.R. Goldwasser, C. Urbina de Navarro, Stud. Surf. Sci. Catal. 135 (2001) 331.
[8] A. Rivera, G. Rodríguez-Fuentes, E. Altshuler, Micropor. Mesopor. Mater. 24 (1998) 51.
[9] A. Rivera, G. Rodríguez-Fuentes, I. García, M. Mir, in: E. Herrero, O. Anunziata, C. Pérez (Eds.), Proceedings of the XV Iberoamerican Symposium on Catalysis, Córdoba, Argentina, vol. 3, 1996, p. 1521.
[10] H. Robson, K.P. Lillerud, Verified Synthesis of Zeolitic Materials, XRD Patterns, second ed., Elsevier, London, 2001, p. 121.
[11] G. Hermeler, J.-Ch. Buhl, W. Hoffmann, Catal. Today 8 (1991) 415.
[12] J.-Ch. Buhl, F. Stief, M. Fechtelkord, Th.M. Gesing, U. Taphorn, C. Taake, J. Alloys Comp. 305 (2000) 93.
[13] R.M. Barrer, J.F. Cole, H. Sticher, J. Chem. Soc (A) (1968) 2475.
[14] E.M. Flaninger, H. Khatami, Adv. Chem. Series 16 (1971) 201.
[15] K. Hackbarth, Th.M. Gesing, M. Fechtelkord, F. Stief, J.-Ch. Buhl, Micropor. Mesopor. Mater. 30 (1999) 347.
[16] A. Burton, M. Feuertein, R. Lobo, J.C. Chan, Micropor. Mesopor. Mater. 30 (1999) 293.
[17] D.W. Piper, B. Fenton, Gut 6 (1965) 506.
[18] J.S. Fordtran, S. Morawski, Ch.T. Richardson, New Engl. J. Med. 288 (1973) 923.